Juvenile Xanthogranuloma of the Head and Neck: Imaging Findings in 11 Cases

François Chalard, Toan Nguyen, Baptiste Morel, Louis-Marie Leiber,
Charles-Joris Roux, Philippe Petit, Gustavo Soto-Ares, Jean Donadieu,
Hubert Ducou Le Pointe

▶ **To cite this version:**

HAL Id: hal-04637076
https://hal.univ-lille.fr/hal-04637076

Submitted on 5 Jul 2024

Juvenile Xanthogranuloma of the Head and Neck: Imaging Findings in 11 Cases

François Chalard, MD,* Toan Nguyen, MD,* Baptiste Morel, MD, PhD,†
Louis-Marie Leiber, MD,‡ Charles-Joris Roux, MD,§
Philippe Petit, MD, PhD,‖ Gustavo Soto Ares, MD,¶
Jean Donadieu, MD, PhD,# and Hubert Ducou le Pointe, MD, PhD*

Background: Juvenile Xanthogranuloma (JXG) is a non-Langerhans cell histiocytosis, occurring mainly in infancy. With an extracutaneous lesion, its diagnosis is difficult, because of a wide clinical spectrum. Here we demonstrate and characterize imaging features of 11 patients with JXG of the head and neck in various locations.

Material and Methods: We recorded clinical data and reviewed all imaging studies of 11 patients with JXG of the head and neck. Ultrasonography (US) alone was performed in 1 patient; MRI alone in 6 patients; US and MRI in 1 patient; and US, CT, and MRI in 3 patients. We evaluated the following characteristics in all studies: location and number of lesions, echogenicity and vascularization on US, density on CT, signal intensity on T_1- and T_2-weighted images, ADC and enhancement on MRI, and tumor boundaries and bone involvement.

Results: Lesions were well-defined in 9 cases, and bone erosion was present in 2. On US, lesions were hypoechoic or hyperechoic and with or without vascularization. On CT, lesions were hyper-dense, with no calcification. On MRI, lesions were mildly hyper-intense or iso-intense on T_1-weighted images in 8 of 9 patients, hypo-intense on T2-weighted images in 7 of 10, low ADC in 7 of 9, and enhancement in 7 of 7.

Conclusions: The diagnosis of extra cutaneous JXG may be proposed, with the following suggestive criteria: age < 1 year, well-defined lesion, mild hyper-intensity on T_1-weighted images, hypo-intensity on T_2-weighted images, low ADC, enhancement, and possible adjacent bone involvement.

Key Words: juvenile Xanthogranuloma, children, head and neck, imaging

(J Pediatr Hematol Oncol 2024;00:000–000)

Juvenile xanthogranuloma (JXG) is a component (C group) of a family of disorders called histiocytoses.[1] It is characterized by the accumulation of cells that are thought to be derived from dendritic cells or macrophages. It is the most common non-Langerhans cell histiocytosis (LCH) in childhood,[2] occurring from the neonatal period to the age of 20 years, but mainly in infants.[3,4] The skin is the most affected site.[3] Cutaneous lesions are well-circumscribed reddish/yellowish nodules or papules located on the head, neck, or trunk.[5] They are benign, with a spontaneous tendency for involution, and without sequelae.[3,5,6] Extracutaneous lesions of JXG have been reported in a limited number of cases, and among such "systemic" cases, the head and neck are the most frequent locations in the subcutaneous fat, deep soft tissue, and organs (eye, paranasal sinuses, nasal fossae, sub-glottis, tongue, cervical spine, muscles, orbit, external auditory canal, tympanic membrane, skull base, and encephalon).[3,7] Outside the head and neck region, JXG may arise from many organs (liver, spleen, lung, kidney, bones, lymph nodes, gastrointestinal tract, testis, adrenal, retroperitoneum, heart, and muscle) and can be unifocal, disseminated, or systemic.[3,5,8–10] The latter clinical presentation is rare (4%) and has a poor prognosis despite appropriate therapy, medical treatment, and surgery. Except for typical cutaneous lesions, the diagnosis of JXG is difficult before pathologic examination because of its rarity and wide clinical spectrum ranging from local to systemic symptoms.

Here, we characterized the imaging features of 11 cases of JXG of the head and neck in various locations.

MATERIAL AND METHODS

From 2006 to 2023, 59 patients with one or multiple nodular lesions of JXG presented to our hospital (Hôpital Armand Trousseau, Paris, France); for the first consultation

TABLE 1. Clinical Data

	Gender	Age (diagnosis/ progression)	Symptoms	Location	No. lesions	Treatment	Outcome
Patient 1	M	2 y	Polyuropolydipsic syndrome, headache	Skin (subpalpebral area)	2	Interferon alpha	Stability
Patient 2	M	17 y	Cheek swelling	Cheek subcutaneous fat	1	Surgery (5 times)/ imatinib then methotrexate/6-mercaptopurine	Recurrences then healing
Patient 3	F	6 mo	Scalp mass	Subcutaneous fat	1	Surgery	Healing
Patient 4	F	Newborn/6 weeks	Multifocal facial swelling, then glaucoma and hyphemia	Subcutaneous fat (eyelids, chin, and forehead), then eye (iris) and subcutaneous fat (face, trunk, inferior limb)	9 then 1	Corticosteroids/vinblastine, then surgery	Progression then healing
Patient 5	F	7 mo	Palpebral swelling	Orbit wall and surrounding soft tissues	1	NA	NA
Patient 6	M	8 mo/4 y	Palpebral swelling, then proptosis	Subcutaneous fat (sub palpebral region) then orbit (extra conic)	1 then 1	Vinblastine then surgery	Progression then healing
Patient 7	F	9 mo	Proptosis, subconjunctival hemorrhage	Left orbit (extra conic)	1	6-mercaptopurine/ vinblastine	Healing
Patient 8	F	9 mo	Poor condition	Brain, bone-marrow, liver, spleen, kidneys, mediastinum	10	Corticosteroids/vinblastine, then cytarabine/ cladribine intracranial)	Progression, then regression and sequala (seizure and speech retardation)
Patient 9	M	6 y	Polyuropolydipsic syndrome, reduced visual acuity, headache, and dysuria	Skin (peri oral region, trunk, buttock), CNS (optic nerve, brainstem, pituitary gland), penis and urethra	> 10 (5	6-mercaptopurine/vinblastine	Healing
Patient 10	F	newborn	Cervical swelling	Mastoid, parotid, external auditory canal, subcutaneous and deep fat	1	Corticosteroids/vinblastine	Progression then stability (residual disease)
Patient 11	F	2 mo	Retro auricular painful mass, then fever and hepatomegaly	Temporal bone (petrous bone, mainly the mastoid and vault)	1	6-mercaptopurine/ vinblastine	Healing

CNS indicates central nervous system; NA, not available.

TABLE 2. Imaging Features

	Tumor boundaries	Bone involvement	US	Doppler	CT	MRI (T_1)	MRI (T_2)	MRI (ADC)	MRI (enhancement)	MRI (other)
Patient 1	well defined	−	NA	NA	NA	NA	Hypointense	NA	+, Homogeneous	
Patient 2	well defined	−	hypo-echoic, heterogeneous	vascularization	NA	NA	NA	NA	NA	
Patient 3	well defined	−	hyper-echoic, heterogeneous	no vascularization	NA	Iso-intense	Hypo-intense	low	NA	
Patient 4	well defined	−	hypo-echoic, homogeneous	no vascularization	hyperdense	iso-intense	Hypo-intense	low	NA	
Patient 5	well defined	+	NA	NA	NA	Mildly hyper-intense	Hypo-intense	low	+, Heterogeneous	
Patient 6	well defined	−	NA	NA	NA	Mildly hyper-intense	Hypo-intense	low	+, Homogeneous	
Patient 7	well defined	−	NA	NA	NA	Mildly hyper-intense	Hypo-intense	low	NA	
Patient 8	well defined	−	NA	NA	NA	Iso-intense	Iso-intense	low	+, Homogeneous	subdural effusion, leptomeningeal enhancement
Patient 9	poorly defined	−	NA	NA	NA	Hypo-intense	Hyper-intense	NA	+, Homogeneous	lack of T1 hyper-signal of the neuro hypophysis
Patient 10	poorly defined	−	hypo-echoic, homogeneous	vascularization	hyperdense	Mildly hyper-intense	Hyper-intense	iso	+, Homogeneous	
Patient 11	well defined	+	hyper-echoic, homogeneous	NA	hyperdense	Mildly hyper-intense	Hypo-intense	low	+, Heterogeneous	

NA indicates not available.
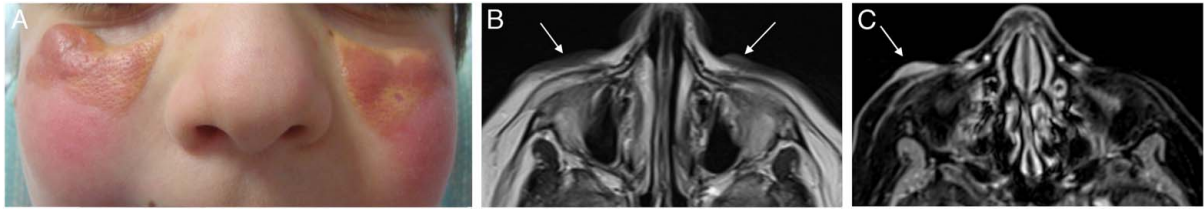
FIGURE 1. Two-year-old boy, skin lesions located below the eyelids. A, The photograph shows bilateral pink-yellow papules B, Axial T_2-weighted image shows bilateral hypo-intense lesions (arrows). C, axial contrast-enhanced fat-suppressed T_1-weighted image showing lesion enhancement (arrow). [full color online]
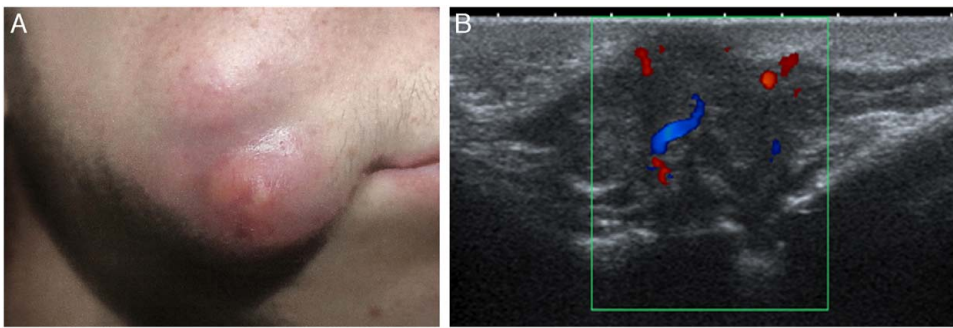
FIGURE 2. Sixteen-year-old boy with a subcutaneous mass of the cheek. A, The photograph shows a subcutaneous lesion, with pink-yellow covering skin B, sonography shows a subcutaneous, heterogeneous, and vascularized tissue mass. [full color online]
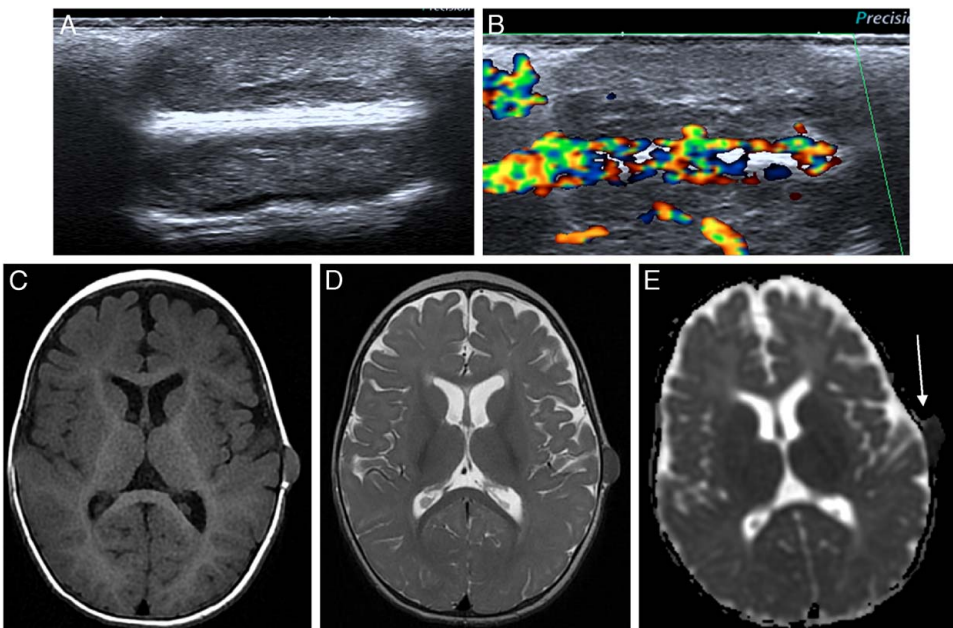
FIGURE 3. Six-month-old girl with subcutaneous ovoid mass of the scalp. A and B, Ultrasonography and color Doppler showing heterogeneous hyper-echogenicity and no vascularization. C, axial T_1-weighted image shows an iso signal. D, axial T_2-weighted image shows a low signal. E, The axial apparent diffusion coefficient (ADC) map shows a low signal (arrow). [full color online]
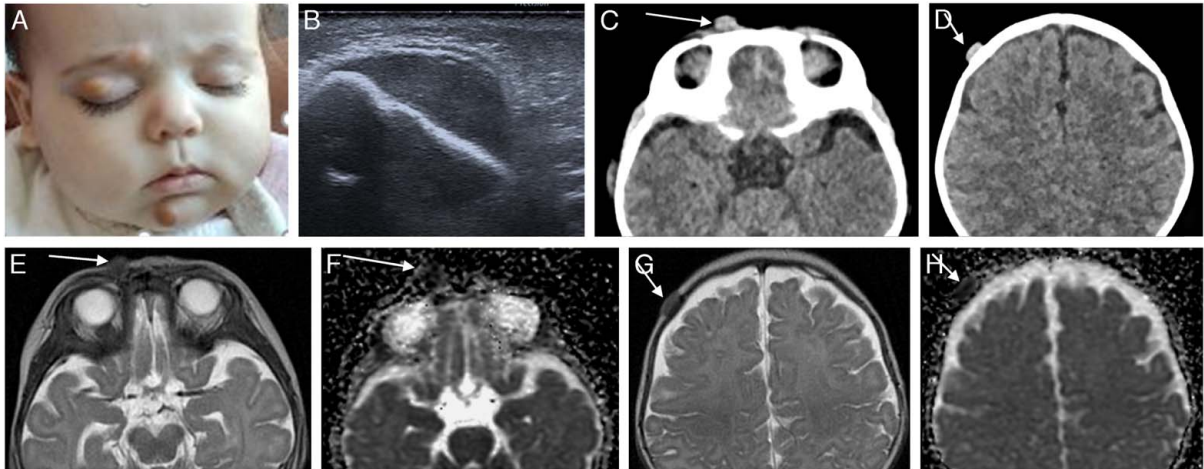
FIGURE 4. Female newborn with 1 sub-periosteal lesion of the skull vault and multiple subcutaneous fat lesions. A, Photograph showing three subcutaneous fat lesions with yellowish covering skin (eyebrows, eyelids, and chin). B, Ultrasonography showing a hypo-echoic, homogeneous sub-periosteal lesion of the skull vault. C and D, CT shows ovoid, hyperdense subcutaneous lesions (arrows). E and G, Axial T_2-weighted images showing hypo-intense round or ovoid subcutaneous lesions (arrows). F and H, Axial ADC maps at the same level show a low signal (arrows). full color online

or referral for specialized care, 11 had JXG in the head and neck region. The following clinical data were recorded for each patient: age, gender, clinical presentation, location and number of lesions, treatment, and outcomes. Each patient underwent at least 1 biopsy. All met the criteria for JXG. Two pediatric radiologists with 30 and 18 years of experience (HDLP and FC, respectively) reviewed all imaging studies. Ultrasonography (US) alone was performed in 1 patient, MRI alone in 6 patients, US and MRI in 1 patient, and US, CT, and MRI in 3 patients. For US,

we compared the echogenicity of lesions to the muscles (for subcutaneous lesions) or cerebellar cortex (for skull base lesions) and noted any vascularization detected on Doppler US. For CT, we visually evaluated the density of the lesions (US) and bone involvement. As we gathered cases from different hospitals, the MRI protocols lacked homogeneity. Nevertheless, each MRI protocol included T_2-weighted images for 10 of 10 patients, T_1-weighted images for 9 of 10 patients, diffusion-weighted imaging, and apparent diffusion coefficient (ADC) mapping for 8 of 10 patients,
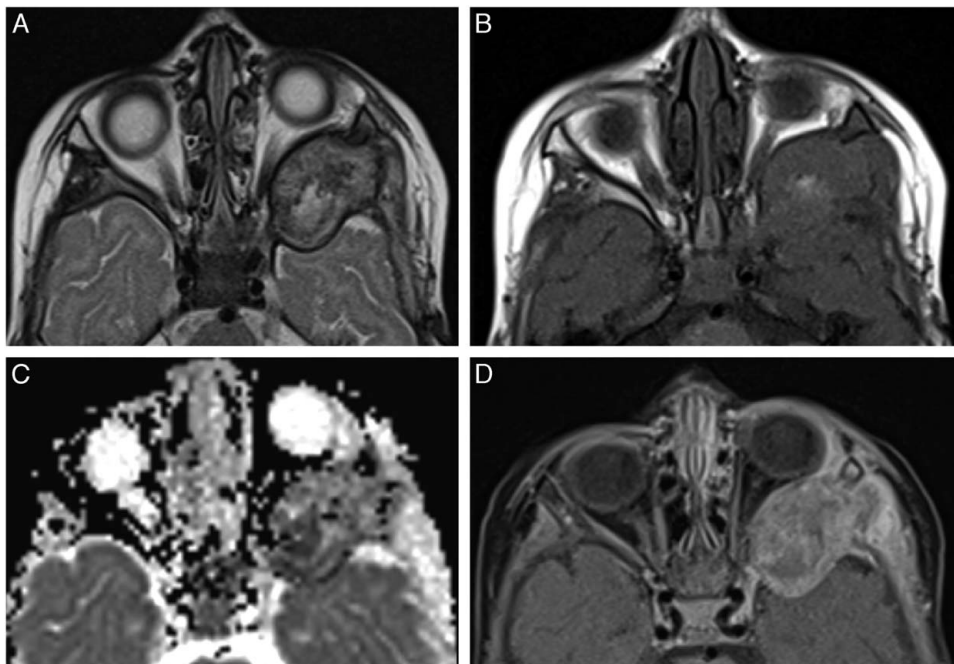
FIGURE 5. Seven-month-old girl with left orbital wall lesion responsible for proptosis and mass effect on the dura matter. A, Axial T_2-weighted image shows a heterogeneous lesion with areas of hypo-intensity. B, axial T_1-weighted image shows a heterogeneous lesion with areas of hyper-intensity. C, axial ADC map shows areas of low ADC within the lesion. D, axial contrast-enhanced fat-suppressed T_1-weighted image shows heterogeneous enhancement.

This paper can be cited using the date of access and the unique DOI number which can be found in the footnotes.
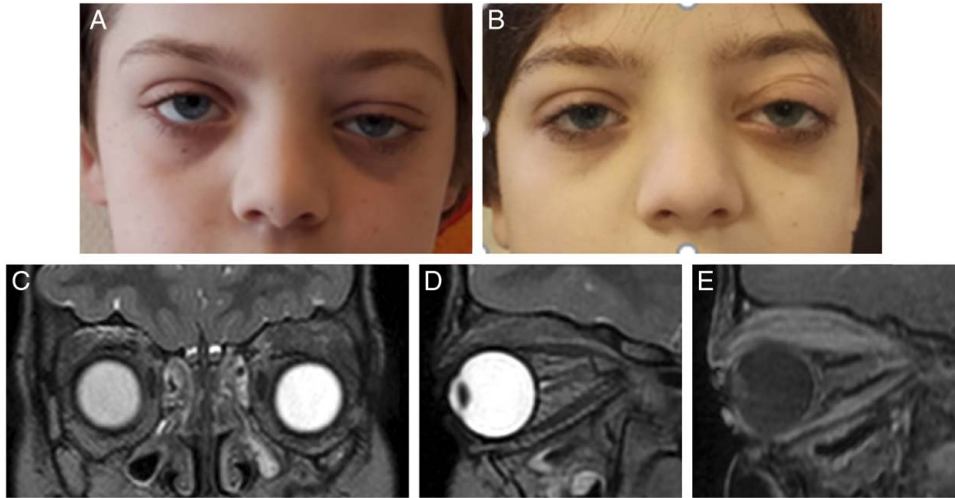
FIGURE 6. An 8-year-old boy with left orbital lesion. A, Photograph showing downward displacement of the left eyeball owing to a lesion located in the upper part of the orbit. B, 18 months later, photograph showing partial regression of the downward displacement of the left eyeball. C and D, Coronal and sagittal T_2-weighted images show a left ill-defined, intraorbital and extraconal mass responsible for the mass effect on the eyeball. E, Sagittal contrast-enhanced fat-suppressed T_1-weighted image showing avid, heterogeneous enhancement. full color online
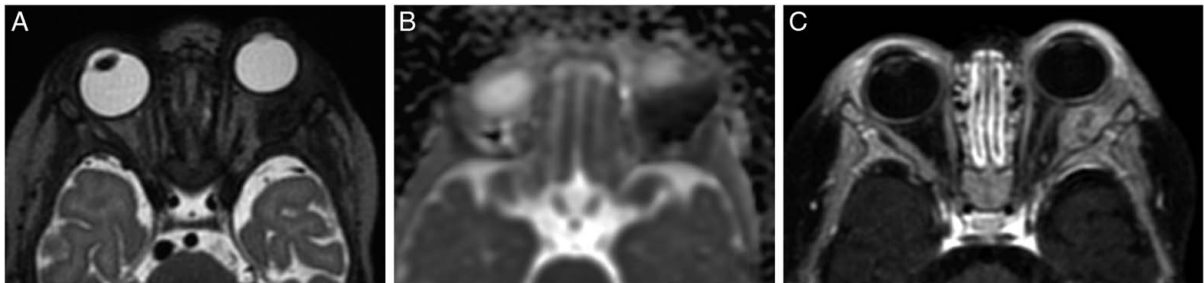
FIGURE 7. Nine-month-old girl with left intraorbital, extraconal lesion responsible for proptosis. A, Axial T_2-weighted image shows a low signal. B, The axial ADC map shows a low signal. C, axial contrast-enhanced fat-suppressed T_1-weighted image shows heterogeneous enhancement.
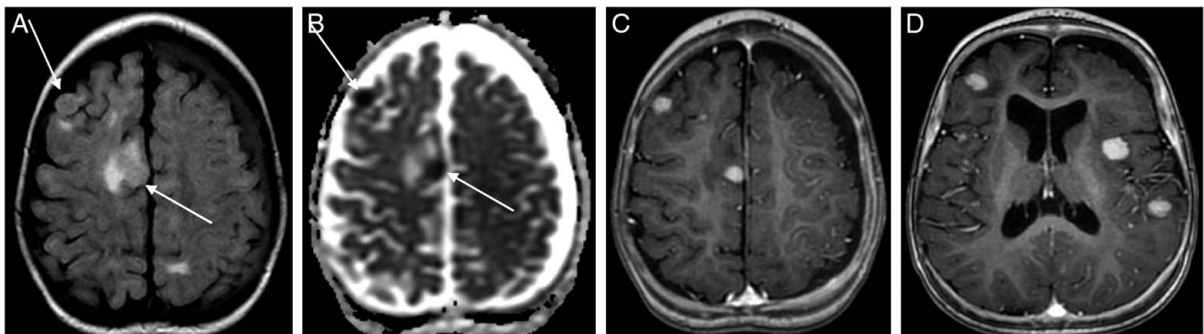
FIGURE 8. Nine-month-old girl with multiple intracranial lesions. A, Axial T_2-FLAIR image showing 2 round cortical lesions (arrows) with iso-signal and mild peripheral edema and left hyper-intense subdural effusion. B, axial ADC map shows a low signal (arrows). C and D, Axial contrast-enhanced T_1-weighted images showing homogeneous lesion and leptomeningeal enhancement.
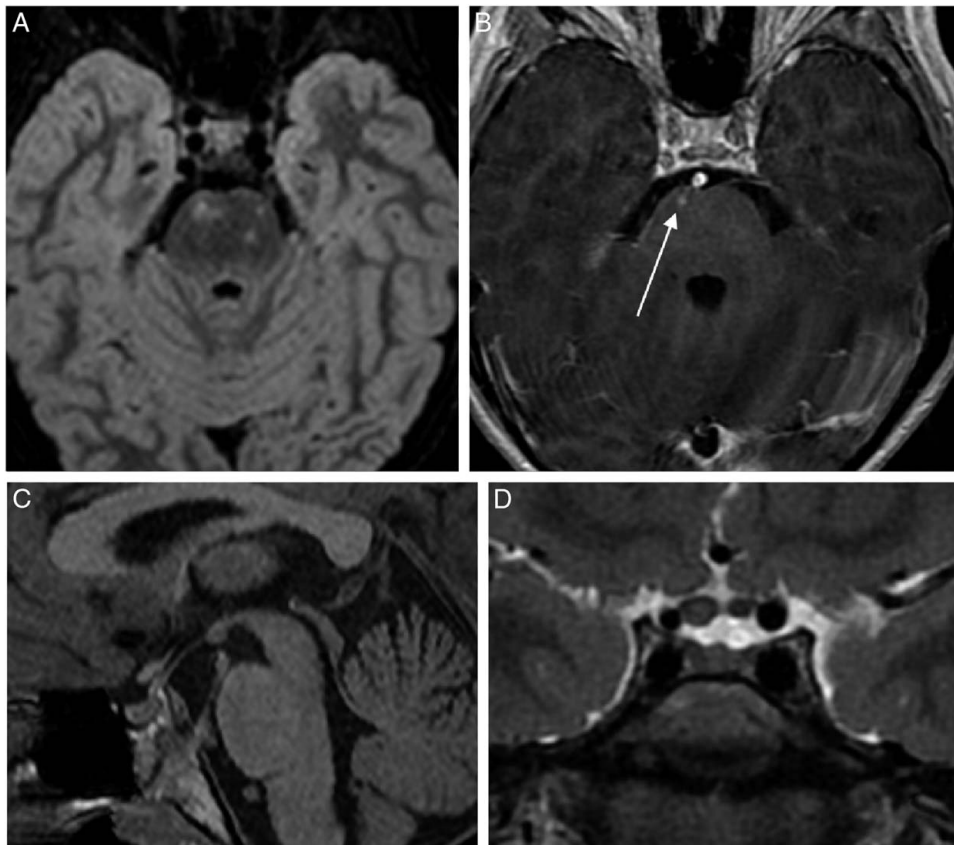
FIGURE 9. Nine-month-old girl with multiple intracranial lesions. A, Axial T_2-FLAIR weighted image shows nodular-punctate hyper-intense lesions of the pons. B, axial contrast-enhanced T_1-weighted image shows a punctate enhancement (arrow). C, Sagittal T_1-weighted image showing lack of hyper-signal of the neuro-hypophysis. D, Coronal T_2-weighted image showing an enlargement and hyper-signal of the right optic nerve.

and T_1-weighted images after gadolinium injection in 7 of 10s. We evaluated lesion signals on T_2- and T_1-weighted images (before and after gadolinium injection) and ADC mapping (compared with the cerebral cortex or contra-lateral symmetrical region, depending on the location). In addition, MRI abnormalities, distinct from nodular lesions, were noted in (the pituitary gland and meningeal spaces).

RESULTS

We reviewed the data of 11 patients with a proven diagnosis of JXG of the head and neck established between 2006 and 2022. Clinical data and imaging features are summarized in Tables 1 and 2, respectively.

The time of imaging ranged from the neonatal period to the age of 17 years. Eight patients were < 1 year old, 1 patient was 2 years old, and 2 patients were > 2 years old. There were 7 females and 4 males.

At diagnosis, the most common clinical presentation was a mass or swelling in 7 cases, sometimes associated with other symptoms (glaucoma, hyphema, proptosis, fever, and hepatomegaly). The 4 other initial presentations were polyuropolydipsic syndrome and headache, poor condition, polyuropolydipsic syndrome, reduced visual acuity, headache and dysuria, proptosis and subconjunctival hemorrhage.

A solitary lesion was initially found in 7 cases, and in one of these cases, an additional lesion appeared > 3 years later. In 1 case, 2 lesions were found at presentation, and in 3 cases, > 9 lesions. In one of the last 3 cases, another lesion appeared secondary (6 wk later). These lesions were in the skin, subcutaneous tissue, parotid gland, external auditory canal, orbit, skull, and intracranial compartment.

More precisely, the distribution of lesions was as follows: Some patients presented lesions in one or more locations:

Skin: 2 cases (isolated lesion: 1 case (Fig. 1A-C); part of systemic disease: 1 case).
Subcutaneous fat: 5 cases (isolated lesion: 2 cases (Fig. 2A, B) and (Fig. 3A-E); with eye [iris] lesions: 1 case (Fig. 4A-H); with orbital lesions: 2 cases)
orbit: 3 cases (bone wall: 1 case (Fig. 5A-D), extraconal soft tissues: 2 cases (Figs. 6A-E and 7A-C))
Central nervous system (CNS): 4 cases, including 2 with intracranial lesions (brain parenchyma and meninges: 1 case (Fig. 8A-D); brainstem, optic nerve, and pituitary gland: 1 case (Fig. 9A-D)) and 2 cases with skull base lesion, one associated with the parotid gland and subcutaneous fat involvement (Figs. 10A-D and 11A-G))
Systemic disease: one case (skin, CNS, and penis)

In all imaging modalities combined, tumors were well defined in 9 cases and poorly defined in 2, and bone erosion was present in 2 cases, one of which involved a large destruction of the mastoid and temporo-occipital vault.

This paper can be cited using the date of access and the unique DOI number which can be found in the footnotes.

FIGURE 10. Female newborn with soft tissue mass in the right cervical region (parotid gland, mastoid, external auditory canal, subcutaneous and deep fat). A, axial fat-suppressed T_2-weighted image shows a hyper-signal. B, axial T_1-weighted image shows a mild hyper-signal. C, The axial ADC map shows a low signal. D, axial contrast-enhanced fat-suppressed T_1-weighted image shows an enhancement.
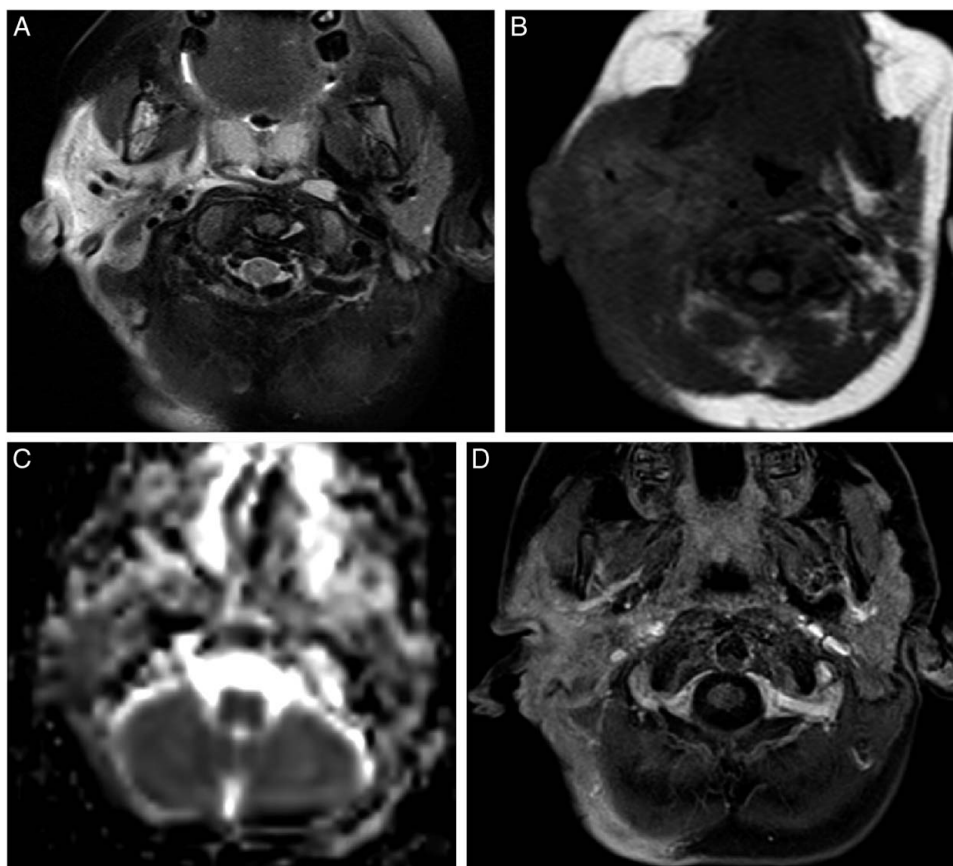
On 5 US and color 4 Doppler US patients, lesions were hypoechoic in 3 patients and hyper-echoic in 2, and vascularization was detected in 2 cases. On 3 CT patients, lesions were hyperdense, with no calcifications or necrosis. On 10 MRI patients, lesions were mildly hyperintense or iso-intense on T_1-weighted images in 8 of 9 patients, hypointense on T_2-weighted images in 7 of 10 patients, had low ADC in 7 of 9 patients, and were enhanced in 7 of 7 patients (homogeneously in 5 patients). One patient was lost to follow-up. The remaining 10 patients underwent treatment: chemotherapy alone in 7 patients, surgery alone in 1 patient, and both surgery and chemotherapy in 2 patients. Various chemotherapy regimens were administered, including corticosteroids, vinblastine, 6-mercaptopurine, cytarabine, cladribine, methotrexate, imatinib, and interferon alpha. The patient outcomes were diverse. Treatment was successful in 7 patients. In the 3 other patients, the disease initially progressed and then stabilized (mastoid, parotid, external auditory canal, subcutaneous and deep fat), stabilized (facial skin), and regressed with sequelae (seizure and speech retardation).

DISCUSSION

Juvenile xanthogranuloma is a rare histiocytic disorder that occurs mainly in infants. Its main location is, by far, the skin (Fig. 1A-C), and it has a predilection for the head,

neck, and trunk regions. Our series of 11 cases confirmed the variety of locations of head and neck JXGs and revealed some imaging characteristics.

Extracutaneous lesions of the head and neck have been reported in numerous anatomic spaces: subcutaneous fat (Figs. 2A, B, 3A-E, 4A-H), paranasal sinuses, nasal cavity, trachea,[11] subglottis, oral cavity and lips,[12–14] orbit, tympanic membrane, external auditory canal, parotid gland, temporal bone, intracranial compartment, and cervical spine.[5] Here, we report the largest series of head and neck JXG at various locations.

Orbital Lesions

Orbital JXG lesions may involve the osseous wall and/or the extraconal soft tissue, including motor ocular muscles, lacrymal glands, and eyelids[15] (Figs. 5A-D, 6A-E, 7A-C).

Orbital Wall Lesions

The main differential diagnoses for orbital bone lesions are LCH and malignant tumors (metastatic neuroblastoma, chloroma, or granulocytic sarcoma). Orbital wall lesions of LCH typically appear as "punched-out" osteolysis, with a small associated soft tissue mass, most often superior or superolateral, and can be multiple.[16] They closely resemble JXG and are difficult to differentiate from LCH, particularly with a solitary lesion. Bone metastasis of
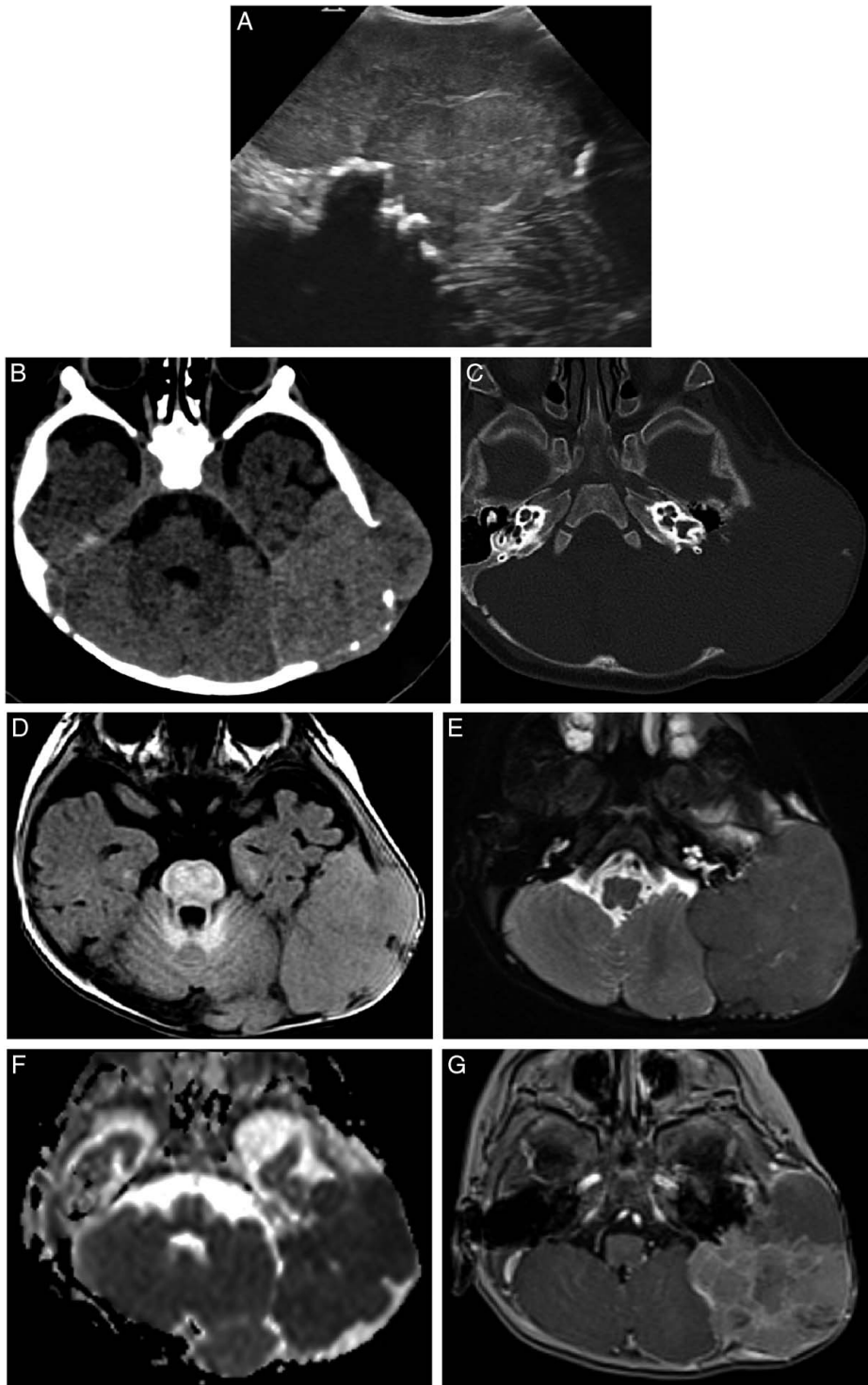
FIGURE 11. Two-month-old girl with a large lesion of the left mastoid and temporo-occipital vault. A, axial ultrasonography shows quite homogeneous echogenicity of the mass. B and C, Axial CT images showing hyperdensity and extensive temporo-occipital bone destruction. D, axial T_1-weighted image shows a mild, homogeneous hyper-signal. E, Axial T_2-weighted image shows a low signal. F, axial ADC map shows a low signal. G, axial contrast-enhanced T_1-weighted image shows heterogeneous enhancement.

neuroblastoma is an invasive and rapidly growing lesion that may be associated with periorbital soft tissue hematoma, with a classic "raccoon eyes" aspect.[17] The signal is commonly heterogeneous on T_2-weighted images and after contrast medium injection because of hemorrhage or necrosis.[18] The detection of the primary tumor is the finding. Chloroma (or granulocytic sarcoma) generally occurs at disease onset or with relapse of acute lymphoid leukemia or myeloproliferative syndrome, although it may be inaugural. It is a homogeneous mass that may involve both bone and soft tissue and tends to encase rather than invade the lacrimal gland and extra-ocular muscles.[19] In addition, bone-marrow replacement may be observed on MRI.[20]

Orbital Soft-tissue Lesion

With orbital soft-tissue lesions, rhabdomyosarcoma, the most common orbital malignancy in childhood, must be considered.[18] It is a rapidly growing tumor with a propensity to arise from the extra-ocular musculature or eyelid.[21] Aggressive bone formation may lead to proptosis and invasion of the adjacent bone. Juvenile Xanthogranuloma may also lead to proptosis or a downward shift of the eyeball, as in 2 of our cases. The optic nerve may be stretched and damaged by proptosis. Rarely, it can also directly involve JXG, as in one of our cases, on one or both sides.[22] Differential diagnoses include inflammatory optic neuritis and optic nerve glioma, with or without neurofibromatosis type 1.

Ocular Lesions

Ocular JXG lesions represent less than 1% of JXG cases and typically occur in infants.[23] It usually involves the iris and, more rarely, the retina or choroid, with spontaneous hyphemia being the most frequent clinical presentation. Second, if left untreated, JXG causes glaucoma and blindness.[24] According to Collie et al[25], ~40% of patients with ocular JXG have multiple cutaneous lesions at the time of diagnosis. However, ocular JXG may be diagnosed with or without cutaneous involvement.[26,27]

Three of our cases illustrated the range of orbital-optical JXG, with lesions of the orbital osseous wall, orbital extraconal space, iris (no available image), and optic nerve.

Mastoid/external Auditory Canal Lesions

Juvenile xanthogranulomas of the external auditory canal[28] and parotid gland[29,30] have been rarely reported and have no specific appearance. Parotid JXG may cause diffuse glandular infiltration, as in one of our cases, or be a focal nodular lesion.[31] The main differential diagnoses of diffuse infiltration of the parotid glands, which is generally bilateral, are lymphoma, leukemia, HIV infection, and systemic disorders (Sjogren's disease, sarcoidosis) (Fig. 10A-D). The general state and extraparotid symptoms contribute to establishing the diagnosis if not known beforehand. Focal, nodular lesions of the parotid gland may be benign or malignant, the most frequent being hemangioma, pleiomorphic adenoma, and mucoepidermoid carcinoma, which have distinct imaging appearances.[32]

Central Nervous System Lesions

Such as juvenile xanthogranuloma of the CNS are rare, ranging from 1% to 2.3%,[4,33] and feature multiple lesions: 76%, according to Ferguson et al[34]; 51%, according to Wang et al[34,35]. The disease can involve supratentorial and infra-tentorial levels[36] and may even have a miliary appearance.[37] Clinical signs are diverse, including seizures, neurological deficits, growth retardation, diabetes insipidus,[38] ocular disturbance,[39] developmental delay, behavioral and memory disorders,[40] and elevated intracranial pressure.[6]

The prognosis of JXG in the CNS is poor when associated with cutaneous lesions or systemic involvement. Indeed, among all head and neck JXG cases, those with intracranial lesions were the most severe. JXG with intracranial involvement is also associated with increased mortality and morbidity.[40,41] Intracranial lesions can be synchronous with skin lesions or can be found months to years later.[39,42,43]

Isolated JXG of the CNS, which is much rarer, consists of a single lesion (65%) and tends to occur more frequently in the skull base,[34] often with a less aggressive clinical course.[44,45] In a review of 39 cases of intracranial JXG reported from 1980 to 2015, Wang et al found that multiple intracranial lesions occurred in 51% and systemic involvement in 58% of cases.[35] The lesion sites were the sellar region, ventricles, cerebellopontine angle, parenchyma (brain much more frequently than cerebellum and brainstem), meninges (dural-cortical lesions and uncommon subdural effusion and lepto meninges lesions), and skull base.

Parenchymal Lesions

Parenchymal JXG typically features multiple nodular enhancing lesions with a mild degree of perilesional edema.[41] It may resemble a wide variety of diseases, which may be difficult to distinguish: ependymoma, glioma, lymphoma, LCH, Rosai-Dorfman-Destombes disease, neurosarcoidosis, and tuberculosis[46,47] (Figs. 8A-D, 9A-D).

In addition, a lack of T_1 hyper signal in the neuro hypophysis, commonly observed in LCH, has been reported in JXG (as in one of our cases).[38]

Moreover, lesions originating from the nerve sheath can mimic schwannoma.[46,47]

Extra-axial Lesions

Dural-based and ventricular lesions are frequently associated with parenchymal involvement.[48,49] The high incidence of ventricular and meningeal lesions may be explained by the presence of macrophages and/or histiocytes in the choroid plexus and meninges.[38] In addition, the dura mater may be involved because of an aggressive, destructive bone JXG.[7,50–52] One case of large infra-tentorial osteodural JXG with a mass effect on the fourth ventricle was reported in a 13-month-old infant, like one of our cases[53] (Figs. 10A-D, 11A-G).

Although dural-based lesions are common in intracranial JXG, leptomeningeal involvement has also been reported in cases of extensive disease (sellar lesions extending to the cavernous sinus, large brainstem lesions, and mild leptomeningeal involvement at the infra-tentorial level)[34] or recurrence.[46]

Dural-based lesions are difficult to differentiate from meningiomas. Although pediatric meningiomas are uncommon, they nonetheless represent the most common dural-based or leptomeninge-based neoplasms in this age group.[54]

Subdural collection is also uncommon in JXG of the CNS, as observed in one of our cases. It is not a hematoma but an effusion related to meningeal involvement, as documented by the analysis of cells from cerebrospinal fluid

in the first published case.[55] In that case, the effusion recurred and responded well to cranial irradiation. In 2008, a case of bilateral, large subdural effusion was reported in a systemic JXG case with brain lesions, but no meningeal anomaly was visible on imaging. After chemotherapy, the brain lesions regressed, but brain atrophy occurred.[40] More recently, a case of subdural collection due to JXG has been reported.[56] The patient initially had shunt-treated hydrocephalus and later exhibited subdural collection, which was presumed to be due to over-shunting. The surgical discovery of a mass lesion and pathologic examination confirmed the presence of JXG.

Spinal Canal/spinal Cord

Juvenile xanthogranulomas may involve the spinal canal and threaten the spinal cord. Both the epidural and intra-dural spaces may be involved as an extension of a spinal lesion[57–59] or as a primary meningeal lesion.[60,61] In addition, intramedullary JXG without adjacent meningeal or bone lesions has been reported.[62]

Disseminated or Systemic Lesions

Disseminated or systemic JXG are uncommon (4% of all cases), have a poor prognosis, and require appropriate therapy, medical treatment, or surgery.[5,42] It may arise from many organs, including the liver, spleen, lung, kidney, bones, lymph nodes, gastrointestinal tract, eye, testis, adrenal gland, retroperitoneum, heart, muscle, and CNS, leading to various symptoms.[4,6,7] We report such a case with involvement of the skin, central nervous system, and penis. Juvenile Xanthogranuloma has been reported in the latter location.[63] In the present case, the lesion was nodular and involved the penile urethra.

Imaging Characteristics

Imaging characteristics of head and neck JXG lesions may have a nonspecific appearance.[8] However, some radiologic characteristics could be identified. On MRI, lesion enhancement is common[7,38,47,48,64–66] and is the most frequent imaging finding by Wang et al, with necrotic, cystic, and hemorrhagic changes less common.[48] Moreover, Su et al reported increased perfusion in the JXG, associated with enhancement.[65] Iso- to hypersignals on T_1-weighted images and isosignals to hyposignals on T_2-weighted images have been noted,[7,30,47,64–68] which Chen et al attributed to the fatty content and attenuated cellularity, respectively, in 27 patients. Nevertheless, such an iso/hyposignal on T_2-weighted images is not pathognomonic, and is also found in fibroblastic and myofibroblastic tumors.[69] Conversely, in a series of 14 cases, Serralach et al found that JXG lesions were iso-intense on T_1-weighted images and iso- or hyper-intense on T_2-weighted images.[70] On diffusion-weighted sequences, a low ADC is generally reported,[7,38,66,68] and Chiba et al considered the intensity on diffusion-weighted imaging to reflect the progression of the lesions. Perilesional edema is absent, mild[38,41,43] and or significant.[48,70,71]

Features of JXG lesions on CT have rarely been reported. In the series by Ginat et al[7], JXG lesions were hypodense in 2 patients who underwent CT. Conversely, intracranial JXG, recently reported by Serrallach et al[70], was homogeneously hyperdense in 4 patients, as in our 2 cases.

In the case of cutaneous or subcutaneous superficial lesions, US with color Doppler is a useful imaging tool. Although it does not allow for establishing the diagnosis of JXG, it readily excludes some differential diagnoses such as dermoid or sebaceous cysts and hypervascularized lesions (typically hemangiomas). Diagnosis is more difficult with neuroblastoma metastasis, muscular and/or fibrous tumors (myofibroma/myofibromatosis, fibrous hamartoma of infancy), or fatty tumors (lipoblastoma).[72]

Indeed, the ultra-sonographic appearance of JXG is a well-defined, hypoechoic tissue nodule without posterior enhancement.[7,57,73–75] On color Doppler US, there is no visible vascularization[65,67] or only low-velocity arterial vessels.[73] Although these imaging characteristics are not pathognomonic elements, they are suggestive clues that we found in our series of head and neck JXG.

CONCLUSIONS

Our series of head and neck JXG reflects the spectrum of presentation of this disease: solitary or multiple cutaneous, subcutaneous, visceral, and even systemic lesions. The diagnosis of cutaneous JXG is strongly suggested by clinical examination and does not require imaging. Regarding other forms of head and neck JXG, the radiologist may be able to suggest this diagnosis based on clinical data (age < 1 y; lesion site: subcutaneous fat, orbit, skull base, dura matter and leptomeninges, ventricles or parenchyma) and imaging characteristics of the lesion(s): Well-defined nodular or large lesion, mild T_1-weighted hyperintensity, T_2-weighted hypointensity, low ADC, enhancement and possible adjacent bone involvement.

REFERENCES

1. Emile JF, Abla O, Fraitag S, et al. Histiocyte Society. Revised classification of histiocytoses and neoplasms of the macrophage-dendritic cell lineages. *Blood.* 2016;127:2672–2681.
2. Weitzman S, Jaffe R. Uncommon histiocytic disorders: The non-Langerhans cell histiocytoses. *Pediatr Blood Cancer.* 2005; 45:256–264.
3. Dehner LP. Juvenile xanthogranulomas in the first two decades of life: a clinicopathologic study of 174 cases with cutaneous and extracutaneous manifestations. *Am J Surg Pathol.* 2003;27: 579–593.
4. Cohen BA, Hood A. Xanthogranuloma: Report on clinical and histological findings in 64 patients. *Pediatr Dermatol.* 1989;6: 262–266.
5. Janssen D, Harms D. Juvenile xanthogranuloma in childhood and adolescence: a clinicopathologic study of 129 patients from the Kiel pediatric tumor registry. *Am J Surg Pathol.* 2005;29: 21–28.
6. Haroche J, Abla O. Uncommon histiocytic disorders: Rosai-Dorfman, juvenile xanthogranuloma, and Erdheim-Chester disease. *Hematology Am Soc Hematol Educ Program.* 2015; 2015:571–578.
7. Ginat DT, Vargas SO, Silvera VM, et al. Imaging features of juvenile xanthogranuloma of the pediatric head and neck. *AJNR Am J Neuroradiol.* 2016;37:910–916.
8. Zaveri J, La Q, Yarmish G, et al. More than just Langerhans cell histiocytosis: a radiologic review of histiocytic disorders. *Radiographics.* 2014;34:2008–2024.
9. Deisch JK, Patel R, Koral K, et al. Juvenile xanthogranulomas of the nervous system: a report of two cases and review of the literature. *Neuropathology.* 2013;33:39–46.
10. Yeh BM, Nobrega KT, Reddy GP, et al. Juvenile xanthogranuloma of the heart and liver: MRI, sonographic, and CT appearance. *AJR Am J Roentgenol.* 2007;189:W202–W204.
11. Naiman AN, Bouvier R, Colreavy MP, et al. Tracheal juvenile xanthogranuloma in a child. *Int J Pediatr Otorhinolaryngol.* 2004;68:1469–1472.
12. Israel MS, Carlos R, Pires FR. Oral juvenile xanthogranuloma: Report of Two Cases. *Pediatr Dent.* 2017;39:238–240.

This paper can be cited using the date of access and the unique DOI number which can be found in the footnotes.

13. Collins L, Banks R, Robinson M. Juvenile xanthogranuloma: Unusual intraoral finding. *Br J Oral Maxillofac Surg*. 2015;53:86–88.

14. Shimoyama T, Horie N, Ide F. Juvenile xanthogranuloma of the lip: Case report and literature review. *J Oral Maxillofac Surg*. 2000;58:677–679.

15. Miszkiel KA, Sohaib SA, Rose GE, et al. Radiological and clinicopathological features of orbital xanthogranuloma. *Br J Ophthalmol*. 2000;84:251–258.

16. Wu C, Li K, Hei Y, et al. MR imaging features of orbital Langerhans cell histiocytosis. *BMC Ophthalmol*. 2019;19:263.

17. D'Ambrosio N, Lyo J, Young R, et al. Common and unusual craniofacial manifestations of metastatic neuroblastoma. *Neuroradiology*. 2010;52:549–553.

18. Rao AA, Naheedy JH, Chen JY, et al. A clinical update and radiologic review of pediatric orbital and ocular tumors. *J Oncol*. 2013;2013:975908.

19. Chung EM, Murphey MD, Specht CS, et al. From the Archives of the AFIP. Pediatric orbit tumors and tumorlike lesions: Osseous lesions of the orbit. *Radiographics*. 2008;28:1193–1214.

20. Porto L, Kieslich M, Schwabe D, et al. Granulocytic sarcoma in children. *Neuroradiology*. 2004;46:374–377.

21. Joseph AK, Guerin JB, Eckel LJ, et al. Imaging findings of pediatric orbital masses and tumor mimics. *Radiographics*. 2022;42:880–897.

22. Daien V, Malrieu Eliaou C, Rodiere M, et al. Juvenile xanthogranuloma with bilateral optic neuritis. *Br J Ophthalmol*. 2011;95:1331–1332.

23. Pantalon A, Ètefǎnache T, Danciu M, et al. Iris juvenile xanthogranuloma in an infant-spontaneous hyphema and secondary glaucoma. *Rom J Ophthalmol*. 2017;61:229–236.

24. Chang MW, Frieden IJ, Good W. The risk intraocular juvenile xanthogranuloma: Survey of current practices and assessment of risk. *J Am Acad Dermatol*. 1996;34:445–449.

25. Collie JS, Harper CD, Fillman EP. Juvenile xanthogranuloma (Nevoxanthoendothelioma, JXG). *In: StatPearls*. Treasure Island (FL): StatPearls Publishing; 2024;10:2020.

26. Hernandez-Martin A, Baselga E, Drolet BA, et al. Juvenile xanthogranuloma. *J Am Acad Dermatol*. 1997;36:355–367.

27. Samara WA, Khoo CT, Say EA, et al. Juvenile xanthogranuloma involving the eye and ocular adnexa: Tumor control, visual outcomes, and globe salvage in 30 patients. *Ophthalmology*. 2015;122:2130–2138.

28. Yoshida GY. Xanthogranuloma of the external auditory canal. *Otolaryngol Head Neck Surg*. 1995;112:626–627.

29. Moukassa D, Maurage CA, Fromentin C, et al. Xanthogranulome juvénile de localisation parotidienne [Juvenile xanthogranuloma localized in the parotid gland]. *Ann Pathol*. 1997;17:113–115.

30. Ho A, Barnes M, McKenney J, et al. Pediatric giant juvenile xanthogranuloma in the parotid gland. *Laryngoscope*. 2011;121:S61–S242. doi:10.1002/lary.22091

31. Dhouib H, Hammami B, Sellami M, et al. Xanthogranulome parotidien de l'adulte [Xanthogranuloma of the parotid gland in adults]. *Rev Stomatol Chir Maxillofac*. 2010;111:337–339.

32. Chalard F, Hermann AL, Elmaleh-Bergès M, et al. Imaging of parotid anomalies in infants and children. *Insights Imaging*. 2022;13:27.

33. Rajaram S, Wharton SB, Shackley F, et al. Intracranial non-Langerhans cell histiocytosis presenting as an isolated intraparenchymal lesion. *Pediatr Radiol*. 2010;40:(suppl 1) S145–S149.

34. Ferguson SD, Waguespack SG, Langford LA, et al. Fatal juvenile xanthogranuloma presenting as a sellar lesion: case report and literature review. *Childs Nerv Syst*. 2015;31:777–784.

35. Wang B, Jin H, Zhao Y, et al. The clinical diagnosis and management options for intracranial juvenile xanthogranuloma in children: Based on four cases and another 39 patients in the literature. *Acta Neurochir (Wien)*. 2016;158:1289–1297.

36. Tamir I, Davir R, Fellig Y, et al. Solitary juvenile xanthogranuloma mimicking intracranial tumor in children. *J Clin Neurosci*. 2013;20:183–188.

37. Lesniak MS, Viglione MD, Weingart J. Multicentric parenchymal xanthogranuloma in a child: case report and review of the literature. *Neurosurgery*. 2002;51:1493–1498.

38. Tan LA, Uy BR, Munoz LF. Recurrent juvenile xanthogranuloma manifesting as diffuse miliary brain lesions. *Br J Neurosurg*. 2014;28:817–818.

39. Chiba K, Aihara Y, Eguchi S, et al. Diagnostic and management difficulties in a case of multiple intracranial juvenile xanthogranuloma. *Childs Nerv Syst*. 2013;29:1039–1045.

40. Boström J, Janssen G, Messing-Jünger M, et al. Multiple intracranial juvenile xanthogranulomas. Case report. *J Neurosurg*. 2000;93:335–341.

41. Auvin S, Cuvellier JC, Vinchon M, et al. Subdural effusion in a CNS involvement of systemic juvenile xanthogranuloma: a case report treated with vinblastin. *Brain Dev*. 2008;30:164–168.

42. Lalitha P, Reddy MCh, Reddy KJ. Extensive intracranial juvenile xanthogranulomas. *AJNR Am J Neuroradiol*. 2011;32:E132–E133.

43. Freyer DR, Kennedy R, Bostrom BC, et al. Juvenile xanthogranuloma: forms of systemic disease and their clinical implications. *J Pediatr*. 1996;129:227–237.

44. Botella-Estrada R, Sanmartín O, Grau M, et al. Juvenile xanthogranuloma with central nervous system involvement. *Pediatr Dermatol*. 1993;10:64–68.

45. Fulkerson DH, Luerssen TG, Hattab EM, et al. Long-term follow-up of solitary intracerebral juvenile xanthogranuloma. Case report and review of the literature. *Pediatr Neurosurg*. 2008;44:480–485.

46. Schultz KD Jr, Petronio J, Narad C, et al. Solitary intracerebral juvenile xanthogranuloma: case report and review of the literature. *Pediatr Neurosurg*. 1997;26:315–321.

47. Pagura L, de Prada I, López-Pino MA, et al. Isolated intracranial juvenile xanthogranuloma. A report of two cases and review of the literature. *Childs Nerv Syst*. 2015;31:493–498.

48. Chen W, Cheng Y, Zhou S, et al. Juvenile xanthogranuloma of central nervous system: imaging of two cases report and literature review. *Radiol Inf Dis*. 2017;4:117–120.

49. Calderon C, Ramsingh A, Pattron R, et al. Multiple intracranial juvenile xanthogranuloma not a straightforward diagnosis (a case report). *Int J Surg Case Rep*. 2021;85:106265.

50. De Paula AM, André N, Fernandez C, et al. Solitary, extracutaneous, skull-based juvenile xanthogranuloma. *Pediatr Blood Cancer*. 2010;55:380–382.

51. Cornips EM, Cox KE, Creytens DH, et al. Solitary juvenile xanthogranuloma of the temporal muscle and bone penetrating the dura mater in a 2-month-old boy. *J Neurosurg Pediatr*. 2009;4:588–591.

52. Wang SN, Lu J. Solitary juvenile xanthogranuloma of temporal bone: a case report. *BMC Pediatr*. 2022;22:87.

53. Yang J, Newbury R, Levy M, et al. Rare presentation of juvenile xanthogranuloma in the posterior fossa of a toddler. *BMJ Case Rep*. 2021;26:e241411.

54. Perry A, Dehner LP. Meningeal tumors of childhood and infancy. An update and literature review. *Brain Pathol*. 2003;13:386–408.

55. Chu AC, Wells RS, MacDonald DM. Juvenile xanthogranuloma with recurrent subdural effusions. *Br J Dermatol*. 1981;105:97–101.

56. Kahn JA, Waltz JT, Eskandari RM, et al. Juvenile xanthogranuloma of the subdural spaces mimicking chronic hematoma with positive FDG uptake on PET: case report. *J Neurosurg Pediatr*. 2020;17:1–5.

57. Bhaisora KS, Jaiswal AK, Mehrotra A, et al. Solitary juvenile xanthogranuloma of the cervical spine in a child: a case report and review of literature. *Asian J Neurosurg*. 2015;10:57.

58. Cao D, Ma J, Yang X, et al. Solitary juvenile xanthogranuloma in the upper cervical spine: case report and review of the literatures. *Eur Spine J*. 2008;17:(suppl 2)S318–S323.

59. Höck M, Zelger B, Schweigmann G, et al. The various clinical spectra of juvenile xanthogranuloma: imaging for two case reports and review of the literature. *BMC Pediatr BMC Pediatr*. 2019;19:128.

60. Shenoy A, Singhal SS, Shinde S. Solitary intraspinal juvenile xanthogranuloma in an infant. *Asian J Neurosurg*. 2018;13: 172–175.

61. Lee SJ, Jo DJ, Lee SH, et al. Solitary xanthogranuloma of the upper cervical spine in a male adult. *J Korean Neurosurg Soc*. 2012;51:54–58.

62. Morice A, Fraitag S, Miquel C, et al. Systemic juvenile xanthogranuloma: a case of spontaneous regression of intra-medullary spinal cord, cerebral, and cutaneous lesions. *J Neurosurg Pediatr*. 2017;20:556–560.

63. Bradford RK, Choudhary AK. Imaging findings of juvenile xanthogranuloma of the penis. *Pediatr Radiol*. 2009;39:176–179.

64. Puerta P, Candela S, Rovira C, et al. Juvenile xanthogranuloma of skull base. Case report and review of the literature. *Acta Neurochir (Wien)*. 2013;155:1039–1040.

65. Su J, Chen N, Yue Q, et al. Multimodel MRI features of an intracranial juvenile xanthogranuloma. *Childs Nerv Syst*. 2019; 35:871–874.

66. He S, Jin K, Deng X, et al. Imaging features of neonatal systemic juvenile xanthogranuloma: a case report and review of the literature. *J Int Med Res*. 2020;48:300060520956416.

67. Myeong HS, Koh EJ, Cheon JE, et al. Intracranial juvenile xanthogranuloma in an infant. *Childs Nerv Syst*. 2021;37: 3265–3269.

68. Chen Y, Yang Z, Shi J, et al. Imaging features of juvenile xanthogranuloma. *Pediatr Radiol*. 2023;53:265–272.

69. Sargar KM, Sheybani EF, Shenoy A, et al. Pediatric fibroblastic and myofibroblastic tumors: a pictorial review. *Radiographics*. 2016;36:1195–1214.

70. Serrallach BL, Kralik SF, Tran BH, et al. Neuroimaging in pediatric patients with juvenile xanthogranuloma of the CNS. *AJNR Am J Neuroradiol*. 2022;43:1667–1673.

71. Miletic H, Röhling R, Stenzel W, et al. 8-year-old child with a lesion in the left nucleus lentiformis. *Brain Pathol*. 2008;18: 598–601.

72. Navarro OM. Pearls and pitfalls in the imaging of soft-tissue masses in children. *Semin Ultrasound CT MR*. 2020;41: 498–512.

73. Niklitschek S, Niklitschek I, González S, et al. Color Doppler sonography of cutaneous juvenile xanthogranuloma with clinical and histologic correlations. *J Ultrasound Med*. 2016; 35:212–213.

74. Martínez-Morán C, Echeverría-García B, Tardío JC, et al. Ultrasound appearance of juvenile xanthogranuloma. *Actas Dermosifiliogr*. 2017;108:683–685; English, Spanish.

75. Wang LM, Chen QH, Zhang YX, et al. Laryngeal juvenile xanthogranuloma: imaging finding. *Int J Pediatr Otorhinolar-yngol*. 2010;74:949–951.

This paper can be cited using the date of access and the unique DOI number which can be found in the footnotes.